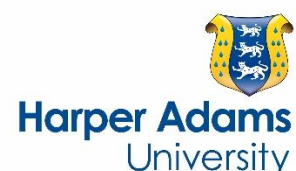


Comparison of methods for estimating the carcass stiffness of agricultural tyres on hard surfaces

by Misiewicz, P.A., Richards, T.E., Blackburn, K. and Godwin, R.A.

Copyright, Publisher and Additional Information: This is the author accepted manuscript. The final published version (version of record) is available online via Elsevier Please refer to any applicable terms of use of the publisher.

DOI: 10.1016/j.biosystemseng.2016.03.001



Misiewicz, P.A., Richards, T.E., Blackburn, K. and Godwin, R.A. 2016. Comparison of methods for estimating the carcass stiffness of agricultural tyres on hard surfaces. *Biosystems Engineering*, 147, pp. 183- 192.

1 Comparison of methods for estimating the carcass 2 stiffness of agricultural tyres on hard surfaces

3
4 P. A. Misiewicz^{a,*}, T. E. Richards^b, K. Blackburn^b and R. J. Godwin^a

5
6 ^aHarper Adams University, Newport, Shropshire, TF10 8NB, UK

7 ^bCranfield University, Cranfield, Bedfordshire, MK43 0AL, UK

8
9 * e-mail of corresponding author: p.misiewicz@iagre.biz

10 11 **Abstract**

12 Loading soil via pneumatic tyres is a major cause of compaction of agricultural soils,
13 which causes damage to the soil-water-air-plant system. The loads applied to the
14 soil and the resulting pressure influences the degree of soil compaction. This study
15 was conducted to determine an effective method to measure the pressure
16 distribution under a selection of pneumatic agricultural tyres. This was conducted
17 initially on a non-deformable surface; a later study will consider pressures within the
18 subsoil. From this the tyre carcass stiffness was determined and methods to predict
19 carcass stiffness were evaluated. Tyre carcass stiffness is defined as an equivalent
20 pressure resulting from the stiffness of the tyre carcass. In order to estimate the
21 carcass stiffness of tyres a number of approaches were considered including: (i)
22 footprint area, (ii) tyre load – deflection, (iii) pressure mapping and (iv) tyre
23 manufacturer's specification methods. Carcass stiffness values obtained from the
24 footprint area method gave results significantly lower (30 – 40%) than those obtained
25 using the pressure mapping system. The method based on the tyre load – deflection
26 characteristics was found to give a better estimation of the tyre carcass stiffness of
27 the smooth rather than the treaded tyre. The technique of using the tyre
28 manufacturer's specification data, where the estimation of the tyre carcass stiffness
29 was calculated using the theoretical load that the tyre could support at zero inflation
30 pressure, produced estimates that were within $\pm 20\%$ of the mean carcass stiffness
31 determined using the pressure mapping system.

32
33 **Keywords:** tyre carcass stiffness; contact pressure; pressure mapping; soil – tyre
34 interactions.

35 **Nomenclature**

36 c_1 tyre carcass stiffness coefficient

37 P_C tyre contact pressure, Pa

38 P_{CS} tyre carcass stiffness pressure, Pa

39 P_i tyre inflation pressure, Pa

40 R^2 coefficient of determination

41

42 **1 Introduction**

43 The steady increase in the power and weight of agricultural machines over recent
44 decades (Horn et al., 2006) has caused a negative effect on soil structure,
45 workability, crop development and yield by increasing soil compaction (Chamen,
46 2011). The heavier and more powerful machines, which have been introduced to
47 improve mechanisation efficiency, have succeeded in reducing costs and improving
48 the timeliness of crop management operations, however, their use may have a
49 negative effect on soils which are susceptible to compaction (Koch et al., 2008).

50

51 The application of load on the soil surface (i.e. on the soil – tyre contact area)
52 transfers stresses through the soil profile which may result in soil compaction if the
53 stress experienced at a given depth exceeds the soil strength. The tyre – soil
54 contact pressure largely determines the degree of surface compaction (Söhne, 1958)
55 and the upper boundary condition for soil stress propagation through the profile
56 depth (Keller and Lamande, 2010). Therefore, the assessment of the contact
57 pressure is of great importance because of its effect on soil compaction. Tyre
58 contact pressure is considered to be an indicator of the potential to cause
59 compaction in the upper layers of the soil (VandenBerg and Gill, 1962; Plackett
60 1984).

61

62 Bekker (1956) noted that the pressure distribution in the case of an ideally elastic
63 tyre on a rigid surface would be uniform and equal to the inflation pressure.
64 However, the presence of tyre treads and carcass stiffness changes this relationship.
65 He presented a simple contact pressure distribution for a solid rubber tyre and a
66 pneumatic tyre, both on a hard surface. The contact pressure distribution for a tyre
67 is not constant; it varies depending on the stiffness of the tyre.

68

69 Soil compaction can result from high contact pressure, low soil strength, or both
70 (Soane et al., 1981). Chancellor (1976), Plackett (1983 and 1986) and Plackett et al.
71 (1987) investigated the factors causing soil compaction and agreed that the major
72 factor was high soil contact pressure. They looked at the contact pressure resulting
73 from agricultural tyres and then related it to the inflation pressure and carcass
74 stiffness. They indicated that mean contact pressure (P_C) could be defined as
75 inflation pressure (P_i) plus carcass stiffness pressure (P_{CS}) :

$$76 \quad P_C = P_i + P_{CS} \quad (1)$$

77 For the purpose of this work, following Bekker (1956), Chancellor (1976) and
78 Plackett (1983), the term tyre carcass stiffness is considered to be an equivalent
79 pressure arising from the stiffness of the tyre carcass. Chancellor (1976) considered
80 different factors affecting the relationship between soil pressure and compactability
81 including soil moisture content, texture, vibration, repeated loading, loading speed
82 and loading period. Unfortunately no experimental results could be found to support
83 his analysis and conclusions.

84

85 The studies by Plackett (1983) provided data for agricultural tyres showing the
86 variation in contact area for increasing loads up to the maximum rated load for the
87 minimum recommended inflation pressure. His research indicated a simple method
88 of measuring hard surface ground contact area and computing the mean contact
89 pressure by dividing the load by the contact area. He suggested that the tyre
90 carcass stiffness contributes to the contact pressure and assumed that this
91 contribution is constant over the tyre deflection range studied. The tyre carcass
92 stiffness was predicted by examining the load – deflection curves for a given tyre.

93

94 In their discussion on pneumatic tyre – soil interactions, Karafiath and Nowatzki
95 (1978) offered a different relationship between the average contact pressure and
96 inflation pressure, presented by Eq. 2, which suggests that the effect of inflation
97 pressure on the contact pressure is affected by a carcass stiffness coefficient (c_1).

$$98 \quad P_C = c_1 P_i + P_{CS} \quad (2)$$

99

100 At present, there is no agreed standard method for determining the contact area or
101 contact pressure of loaded agricultural tyres. With the general increase in the size
102 and power of machines and a better understanding of the factors affecting plant
103 growth, there is a need for further detailed research on soil contact pressure caused
104 by vehicular traffic to aid tyre selection.

105

106 This manuscript describes an investigation of contact pressures resulting from
107 loaded agricultural tyres on hard surfaces, which should enable improved tyre
108 selection for better soil management. A study on the effect of tyres and rubber
109 tracks at high axle loads on soil compaction by Ansorge and Godwin (2007)
110 emphasised the importance of contact pressure distribution with respect to changes
111 in soil compaction. They argued that a uniform pressure distribution is essential to
112 minimise soil compaction, which was supported by the results of Schjonning et al.
113 (2008).

114

115 As tyre contact pressure is a combination of tyre inflation pressure and carcass
116 stiffness (Chancellor, 1976; Plackett, 1983), the objective of this article is to:-

- 117 i. Determine an effective method to measure the contact pressure distribution
118 from pneumatic agricultural tyres on a hard surface,
- 119 ii. Estimate tyre carcass stiffness and
- 120 iii. Develop and assess potential predictive methods for tyre carcass stiffness
121 estimation.

122

123 **2 Materials and Methods**

124 In order to determine the carcass stiffness of a tyre on hard surfaces, a number of
125 approaches were considered including:

- 126 i. The footprint area method, using an ink marker, to estimate the size of the
127 contact patch and hence the mean contact pressure,
- 128 ii. The tyre load – deflection method,
- 129 iii. The pressure mapping method to measure the pressure distribution using a
130 commercial pressure mapping system,
- 131 iv. Tyre manufacturer’s specification methods (two variants).

132

133 The technique using the footprint area, proposed by Plackett (1983), is based on the

134 assumption that tyre carcass stiffness is a constant value for a tyre (Bekker, 1956
135 and Chancellor, 1976) and is calculated as the difference between the mean contact
136 pressure and tyre inflation pressure. Tyre contact area was found by loading tyres,
137 coated in black ink, onto a white card placed on a steel plate. The mean and
138 maximum contact pressures under a tyre were calculated by dividing tyre load by the
139 projected area and tread contact area, respectively. The projected contact area was
140 obtained by loading and rotating a tyre a number of times, while the tread contact
141 area was given by a single ink print.

142

143 Plackett (1983) also predicted the contribution of the tyre carcass stiffness by
144 examining the load – deflection characteristic of a tyre at a range of inflation
145 pressures from which the tyre sidewall stiffness could be estimated. Using this
146 method, the maximum vertical deflection of tyres loaded onto a steel plate was
147 measured using two drawstring potentiometers, one on each side of the tyre, which
148 were connected between the axle and the steel plate. The relationships were then
149 plotted as load vs. deflection (Fig. 1). As the tyre inflation pressure decreases, the
150 slope of the load – deflection curve also decreases. If a tyre has zero carcass
151 stiffness, then the slope of the load – deflection relationship would be zero at zero
152 inflation pressure, as the carcass would not support any load. Therefore, plotting the
153 slope of the load – deflection curve against inflation pressure, as shown in Fig. 2,
154 and extrapolating the relationship to the inflation pressure axis gives an estimation of
155 the carcass strength at zero inflation pressure (abscissa) and the pressure at which
156 the carcass strength is zero (ordinate). Plackett (1983) suggested that the negative
157 value of the inflation pressure at zero slope (load – deflection) is an indication of the
158 tyre carcass stiffness.

159

160 Directly measuring contact pressure is the most fundamental approach for
161 determining carcass stiffness. The mean and maximum contact pressures are
162 determined using a pressure mapping system and mean and maximum tyre carcass
163 stiffness are calculated as the differences between the mean and maximum contact
164 pressures and tyre inflation pressure, respectively. The use of a pressure mapping
165 system (Tekscan System, I-Scan version, Tekscan Inc., South Boston, Mass., USA)
166 allows the real-time pressure distribution to be viewed and recorded across the
167 contact patch using a sensor array. The system had not been previously used in

168 contact pressure experiments with agricultural tyres and for its use here required a
169 bespoke calibration to be developed. This employed, both, an individual and multi-
170 point calibration of each sensing element and the rejection of faulty sensing
171 elements (Misiewicz et al., 2015). This method enabled both the tyre contact area
172 and the contact pressure distribution to be measured with sensors placed on a
173 smooth sheet of aluminium (1.5 m long x 1.5 m wide x 10 mm thick) located on a 70
174 mm thick steel plate. The sensors were covered with a layer of thin plastic film to
175 prevent damage by the tyre treads. The tyres were loaded onto the hard surface
176 and rolled freely straight-ahead at a constant speed of 0.3 km h⁻¹ and the contact
177 pressure was logged at a sampling rate of 100 Hz.

178 The experiments were conducted on a hard surface in the soil bin laboratory,
179 developed by Godwin et al. (1987), which provided controlled conditions for tyre
180 evaluation. The soil tank was 20 m long, 0.8 m deep and 1.65 m wide as shown in
181 Fig. 3. The hard surface experiments required preparation of dense soil conditions
182 in the soil bin onto which three 70 mm thick steel plates (2.5 m long x 1.5 m wide)
183 were placed to provide a non-deformable flat and uniform surface. Then, depending
184 on the method of tyre evaluation, white paper sheets, tyre deflection sensors or
185 pressure sensors were placed on the plates and the tyres were loaded either
186 statically or dynamically. Figure 4 shows the smooth (tread mechanically removed)
187 and treaded Trelleborg T421 Twin Implement 600/55-26.5 166A8 tyres studied. They
188 were used as single free rolling tyres at a range of loads and inflation pressures up
189 to the manufacturer's recommendations for a maximum speed of 10 km h⁻¹.

190

191 A predictive technique, suggested by Godwin (personal communication, 2007), was
192 investigated to determine the feasibility of using currently available manufacturer's
193 data to estimate tyre carcass stiffness. To develop this possible method, tyre
194 manufacturer's specification graphs were used to estimate tyre stiffness by plotting
195 the maximum load against inflation pressure. This relationship was extrapolated
196 using a linear function in order to provide two selected values:

- 197 a. The "negative" inflation pressure at zero load
- 198 b. The load at zero inflation pressure

199 Where:

- 200 a. The "negative" inflation pressure at zero load, gives a residual tyre stiffness that

201 could be an indicator of tyre carcass stiffness. This method is very simple, as it
202 requires only data already published by the tyre manufacturer.

203

204 b. The load that can be supported by a tyre at zero inflation pressure provides data
205 that can be converted into a pressure applied over the tyre contact area. This
206 method of tyre stiffness estimation requires the tyre contact area to be measured at
207 the recommended load and inflation pressure.

208

209 **3 Results and discussion**

210

211 **3.1 The footprint area method**

212 The mean contact pressures calculated according to the footprint area were found to
213 be greater than the inflation pressures for both tyres (Figs. 5 and 6). An increase in
214 inflation pressure resulted in a significant rise in the mean contact pressure for both
215 smooth and treaded tyres. The load did not have an effect on the mean contact
216 pressure for either the smooth or treaded implement tyres, while the interaction
217 between the tyre load and inflation pressure was significant at the 95% confidence
218 level (Misiewicz, 2010).

219

220 The difference between the mean contact pressure and tyre inflation pressure for the
221 smooth implement tyre (Fig. 5) was found to vary from 0.1×10^5 Pa to 0.5×10^5 Pa
222 with a mean value of 0.28×10^5 Pa. The difference between the mean contact
223 pressure, based on the projected area, and the inflation pressure for the treaded
224 implement tyre was found to vary as a function of tyre inflation pressure with a mean
225 value of 0.41×10^5 Pa (Fig. 6a). The difference between the mean contact pressure,
226 according to the tread contact area, and tyre inflation pressure was found to be
227 greater and varied from 2.75×10^5 Pa to 5.5×10^5 Pa depending on tyre inflation
228 pressure with a mean value of 4.38×10^5 Pa (Fig. 6b). The relationships presented in
229 both Figs. 5 and 6, follow the model of Karafiath and Nowatzki (1978), where the c_1
230 is not equal to 1.

231

232 **3.2 Tyre load - deflection method**

233 Figure 7 shows the data collected for both the smooth and treaded implement tyres.

234 An increase in tyre load results in an increase in tyre deflection for both tyres and the
235 slope of the load – deflection curve increases as inflation pressure increases. The
236 slopes of the load – deflection curves for the same inflation pressures are
237 approximately the same for the smooth and treaded tyres. However, as the smooth
238 implement tyre was found to deflect more than the treaded tyre the intercepts of the
239 relationships differ. Therefore, it was shown that tyre tread has an effect on tyre
240 vertical deflection; however, it does not have an effect on the slope of the load –
241 deflection characteristic; this was expected, as it is the tyre sidewalls that deflect.
242 The slopes of these relationships were plotted against inflation pressure, as shown in
243 Fig. 8 and were found to be linear (coefficient of determination (R^2) = 0.9957 and
244 0.9853, respectively). Extrapolation of the trends to the intercept of the inflation
245 pressure axis gave predicted carcass stiffness of 0.83×10^5 Pa for both the smooth
246 and treaded implement tyres.

247

248 **3.3 The pressure mapping method**

249 Figures 9 and 10 show the mean and maximum contact pressure vs. inflation
250 pressure respectively for both the smooth and the treaded tyre obtained using the
251 pressure mat. The data confirmed that as inflation pressure increases there is an
252 increase in both the mean and maximum contact pressure for both smooth and
253 treaded tyres. Both the mean and maximum contact pressures were found to be
254 higher than the tyre inflation pressure over the range studied. As expected the effect
255 of the tyre tread significantly increased both the mean and maximum contact
256 pressures at the 95% confidence level. The linear regression analyses confirmed
257 that both tyre load and inflation pressure had significant effects on the mean and
258 maximum contact pressure of the smooth tyre. For the treaded tyre, only the
259 inflation pressure had an influence on the resulting contact pressures. Statistical ‘t’
260 tests showed that the contact pressure did not increase at the same rate as tyre
261 inflation pressure, therefore, the effect of inflation pressure on the contact pressure is
262 affected by the c_1 (not equal to 1), also in agreement with Karafiath and Nowatzki
263 (1978).

264

265 The difference between the mean contact pressure and inflation pressure,
266 considered as mean carcass stiffness, for the smooth tyre varied between 0.3×10^5

267 Pa and 0.7×10^5 Pa and the maximum carcass stiffness varied between 3×10^5 Pa
268 and 5×10^5 Pa. The overall mean values of mean and maximum carcass stiffness of
269 the smooth implement tyre were found to be 0.44×10^5 Pa and 3.81×10^5 Pa,
270 respectively. For the rated loads and inflation pressures, the means of the mean and
271 maximum carcass stiffness were 0.54×10^5 Pa and 4.46×10^5 Pa, respectively.

272

273 The carcass stiffness of the treaded implement tyre was found to be significantly
274 greater than the carcass stiffness of the smooth tyre. The mean values were found
275 to vary between 2.0×10^5 and 3.2×10^5 Pa and the maximum carcass stiffness
276 varied between 5.9×10^5 and 8.4×10^5 Pa. The overall mean values of mean and
277 maximum carcass stiffness of the treaded implement tyre tested were equal to $2.51 \times$
278 10^5 Pa and 7.16×10^5 Pa, respectively. For the rated loads and inflation pressures,
279 the means of the mean and maximum carcass stiffness were 2.53×10^5 Pa and 7.25
280 $\times 10^5$ Pa, respectively.

281

282 **3.4 Tyre manufacturer's specification method**

283 The load vs. inflation pressure data for the implement tyre from the tyre
284 manufacture's specification for a range of loading cycles and speeds was considered
285 by extrapolating the relationships using a linear regression analyses. The
286 relationships were found to be highly linear with the $R^2 > 0.999$ (Misiewicz, 2010).
287 Extrapolating these relationships produces a range of points on the negative inflation
288 pressure axis that tend to converge. Using the inflation pressure at zero load for a
289 free rolling implement tyre at a speed of 10 km h^{-1} , as shown in Fig. 11 as an
290 example of the implied carcass stiffness and as the closest speed to the speed used
291 in the experiment, the results were found to be 0.79×10^5 Pa.

292

293 The carcass stiffness was also estimated based on the tyre load which can be
294 carried by a non-inflated tyre (Fig. 11). It was observed that tyres maintain a near
295 constant contact area, when they are loaded with the recommended load for a given
296 inflation pressure, according to tyre manufacture specifications (Misiewicz, 2010).
297 Therefore, only one contact area experimental test for a tyre is required or, in the
298 future, it could be provided in the tyre manufacturer's specification data. The contact
299 areas, required in order to convert the load that the tyres are able to carry with no
300 pressure, were determined using the pressure mapping system. The carcass

301 stiffnesses of the free rolling implement tyre at 10 km h⁻¹ were found to be:

- 302 • for the smooth tyre: 0.65 x 10⁵ Pa (mean contact area 0.26 m²)
- 303 • for treaded tyre: 2.12 x 10⁵ Pa (mean tread contact area 0.08 m²)

304

305 **3.5 Comparison of results**

306 Table1 and Fig. 12 compare the results obtained for different methods of carcass
307 stiffness determination. The carcass stiffness values provided by the footprint area
308 method were considerably lower than the results obtained using the pressure
309 difference method using the pressure mapping system. The results were
310 approximately 30 – 40% lower than the tyre carcass stiffness obtained by the
311 pressure mapping method, so they should not be used for estimating mean contact
312 pressure on a hard surface. This indicates that the contact areas provided by the
313 footprint area method include areas where the tyres have contact with the surface
314 but transfer little or no load, which leads to an underestimate of the mean contact
315 pressure. The methods based on tyre load – deflection and tyre manufacturer
316 specification data based on the inflation pressure at zero load, produced estimates of
317 the mean tyre carcass stiffness that are closer to those measured using the pressure
318 mapping method for the smooth tyre. The estimation of the tyre carcass stiffness
319 according to the theoretical load that the tyre is able to sustain at zero inflation
320 pressure, gave the closest agreement with the mean carcass stiffness of both the
321 smooth and treaded tyres studied, this was found to lie within ± 20% of that
322 determined using the pressure mapping system. Hence, the method based on tyre
323 manufacturer data using the load at zero inflation pressure is recommended as a
324 simple indicator of the mean tyre carcass stiffness in the absence of equipment to
325 record actual contact pressure. To make this method easier the intercept data for
326 the zero load and the rated contact area should be included in the tyre
327 manufacturer's specification.

328

329 **4 Conclusions**

330 Using the pressure mapping method, where the mean and maximum contact
331 pressures of the tyre footprint were determined, allowed the following methods of
332 carcass stiffness estimation to be evaluated:

- 333 i. The footprint area method to estimate the size of the contact patch and

- 334 hence the mean contact pressure,
335 ii. Tyre load – deflection method,
336 iii. Tyre manufacturer’s specification method.

337 Carcass stiffness values obtained using the footprint area method were significantly
338 less (30 – 40%) than the tyre carcass stiffness values obtained by using the pressure
339 mapping method. The methods based on the tyre load – deflection and tyre
340 manufacturer’s specification based on the inflation pressure at zero load gave a
341 better estimates of the mean tyre carcass stiffness of the smooth tyre. The method
342 based on the tyre manufacturer’s specification data, where the estimate of the tyre
343 carcass stiffness was according to the theoretical load that the tyre is able to sustain
344 at zero inflation pressure, gave the best agreement with the mean carcass stiffness
345 of both the smooth and treaded tyres which was found to be within $\pm 20\%$ of that
346 recorded using the pressure mapping method.

347
348 The pressure mapping method can be used to determine the maximum carcass
349 stiffness, which was found to be approximately 3 times the mean carcass stiffness of
350 the treaded tyre.

351
352 The tyre tread of the Trelleborg 600/55-26.5 tyre has a significant effect on the
353 contact area; mean and maximum contact pressure and the resulting carcass
354 stiffness on a hard surface.

355
356 In order to provide practical assistance in the selection of tyres with the lowest mean
357 contact pressure, the carcass stiffness estimated from the tyre manufacturer
358 specification data should be used. To make this method easier the intercept data for
359 the zero load and the rated contact area should be included in the tyre
360 manufacturer’s specification.

361
362 **References**

363 Ansoorge, D., & Godwin, R.J. (2007). The effect of tyres and a rubber track at high
364 axle loads on soil compaction, Part 1: Single axle-studies. *Biosystems Engineering*,
365 98 (1), 115 – 126.

366 Bekker, M.G. (1956). *Theory of land locomotion: the mechanics of vehicle mobility*.
367 The University of Michigan Press, USA.

- 368 Chamen, W.C.T. (2011). The mechanisation, economics and agronomic effects of
369 field traffic management on cropping systems. PhD thesis, Cranfield University,
370 Cranfield, UK.
- 371 Chancellor, W.J. (1976). Compaction of soil by agricultural equipment. Bulletin 1881.
372 Div. Agric. Sci. University of California, Davis, USA.
- 373 Godwin, R.J., Magalhaes, P.S.G., Miller, S.M, & Fry, R.K. (1987). Instrumentation to
374 study the force systems and vertical dynamic behaviour of soil-engaging implements.
375 *Journal of Agricultural Engineering Research*, 36, 301 – 310.
- 376 Koch, H. J., Heuer, H., Tomanova, O., & Marlander, B. (2008). Cumulative effect of
377 annually repeated passes of heavy agricultural machinery on soil structural
378 properties and sugar beet yield under two tillage systems. *Soil & Tillage Research*,
379 101, 69 - 77.
380. Horn, R., Fleige, H., Peth, S., & Peng, X. (2006). Soil management for sustainability,
381 *Advances in GeoEcology. The 17th Triennial International Soil Tillage Research*
382 *Conference, CATENA VERLAG GMBH, Kiel, Germany, 28 August – 3 September*
383 *2006.*
- 384 Karafiath, L.L., & Nowatzki, E.A. (1978). Soil mechanics for off-road vehicle
385 engineering. 1st edition, Trans Tech Publications, Germany.
- 386 Keller, T. and Lamandé, M. (2010). Challenges in the development of analytical soil
387 compaction models. *Soil and Tillage Research*, 111, 54 – 64.
- 388 Misiewicz P.A., Blackburn, K., Richards, T.E., Brighton, J.L., & Godwin, R.J. (2015).
389 The evaluation and calibration of pressure mapping system for the measurements of
390 the pressure distribution. *Biosystems Engineering*, 130, 81 – 91.
- 391 Misiewicz, P.A. (2010). The evaluation of the soil pressure distribution and carcass
392 stiffness resulting from pneumatic agricultural tyres. PhD Thesis, Cranfield
393 University, Cranfield, UK.
- 394 Plackett, C.W. (1986). Instrumentation to measure the deformation and contact
395 stress of pneumatic tyres operating in soft soil. Divisional Note DN 1322. National
396 Institute of Agricultural Engineering, Silsoe, England.
- 397 Plackett, C.W. (1984). The ground pressure of some agricultural tyres at low load
398 and with zero sinkage. *Journal of Agricultural Engineering Research*, 29, 159 – 166.
- 399 Plackett, C.W. (1983). Hard surface contact area measurement for agricultural tyres.
400 Divisional Note DN 1200. National Institute of Agricultural Engineering, Silsoe,
401 England.
- 402 Plackett, C.W., Clemens K., Dwyer, M. J., & Febo, P. (1987). The ground pressure of
403 agricultural tyres. AFRC Institute of Engineering Research, Report No.49.

404 Schjonning, P., Lamande, M., Togersen, F.A., Arvidsson, J., & Keller, T. (2008).
405 Modelling effects of tyre inflation pressure on the stress distribution near the soil –
406 tyre interface. *Biosystems Engineering*, 99, 119 – 133.

407 Soane, B.D, Blackwell, P.S., Dickson, J.W., & Painter, D.J. (1981). Compaction by
408 agricultural vehicles: a review, I. Soil and wheel characteristics. *Soil Tillage*
409 *Research*, 1, 207 – 237.

410 Söhne, W.H. (1958). Fundamentals of pressure distribution and soil compaction
411 under tractor tyres. *Agricultural Engineering*, 39, 276 – 281, 290.

412 Trautner, A. (2003). On soil behaviour during field traffic. PhD thesis, Swedish
413 University of Agricultural Sciences, Uppsala.

414 VandenBerg, G.E., & Gill, W.R. (1962). Pressure distribution between a smooth tyre
415 and the soil. *Transactions of ASAE*, 5, 2, 105 – 107.

416

417

418

419

420

421

422

423 **Figures:**

424 Fig. 1. Load vs. deflection curves for a tyre at a range of inflation pressures (redrawn
425 from Plackett, 1983)

426 Fig. 2. Carcass stiffness estimated from the inflation pressure vs. slope of load –
427 deflection curves for three tyres (redrawn from Plackett, 1983)

428 Fig. 3. Soil bin laboratory (a: soil surface preparation, b: pressure mapping system
429 placed on the steel plates)

430 Fig. 4. Smooth (a) and treaded (b) Trelleborg T421 Twin Implement 600/55-26.5
431 tyres

432 Fig. 5. Mean contact pressure vs. inflation pressure for the smooth 600/55-26.5
433 implement tyre from the footprint area method (*the single marker centred within
434 each circle indicates a data point for a rated combination of load and inflation
435 pressure)

436 Fig. 6. Mean and maximum contact pressure vs. inflation pressure for the 600/55-
437 26.5 treaded implement tyre from the footprint area method (*the single marker
438 centred within each circle indicates a data point for a rated combination of load and
439 inflation pressure)

440 Fig. 7. Load vs. deflection curves – smooth (a) and treaded (b) 600/55-26.5
441 implement tyre (*the single marker centred within each circle indicates a data point
442 for a rated combination of load and inflation pressure)

443 Fig. 8. Inflation pressure vs. slope of load – deflection curve – smooth (left) and
444 treaded (right) 600/55-26.5 implement tyre

445 Fig. 9. Mean and maximum contact pressures vs. tyre inflation pressure for the
446 smooth 600/55-26.5 implement tyre for a range of safe working loads based on the
447 pressure mapping system (*the single marker centred within each circle indicates a
448 data point for a rated combination of load and inflation pressure)

449 Fig. 10. Mean and maximum contact pressures vs. tyre inflation pressure for the
450 treaded 600/55-26.5 implement tyre for a range of safe working loads based on the
451 pressure mapping system (*the single marker centred within each circle indicates a
452 data point for a rated combination of load and inflation pressure)

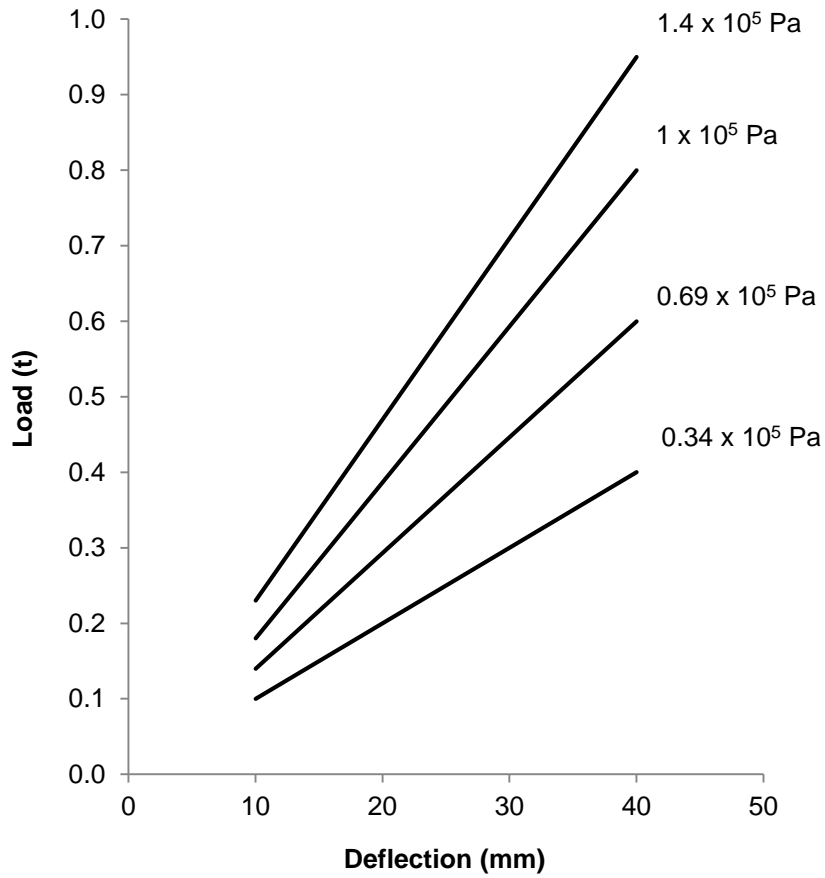
453 Fig. 11. Tyre manufacturer's specification data showing the inflation pressure vs.
454 load with a linear regression function for the 600/55-26.5 implement tyre (free rolling
455 at 10 km h⁻¹ speed)

456 Fig. 12. Comparison of the mean estimated tyre carcass stiffness values with

457 absolute measured values for the Trelleborg T421 Twin Implement 600/55-26.5 tyres
458

459 **Tables:**

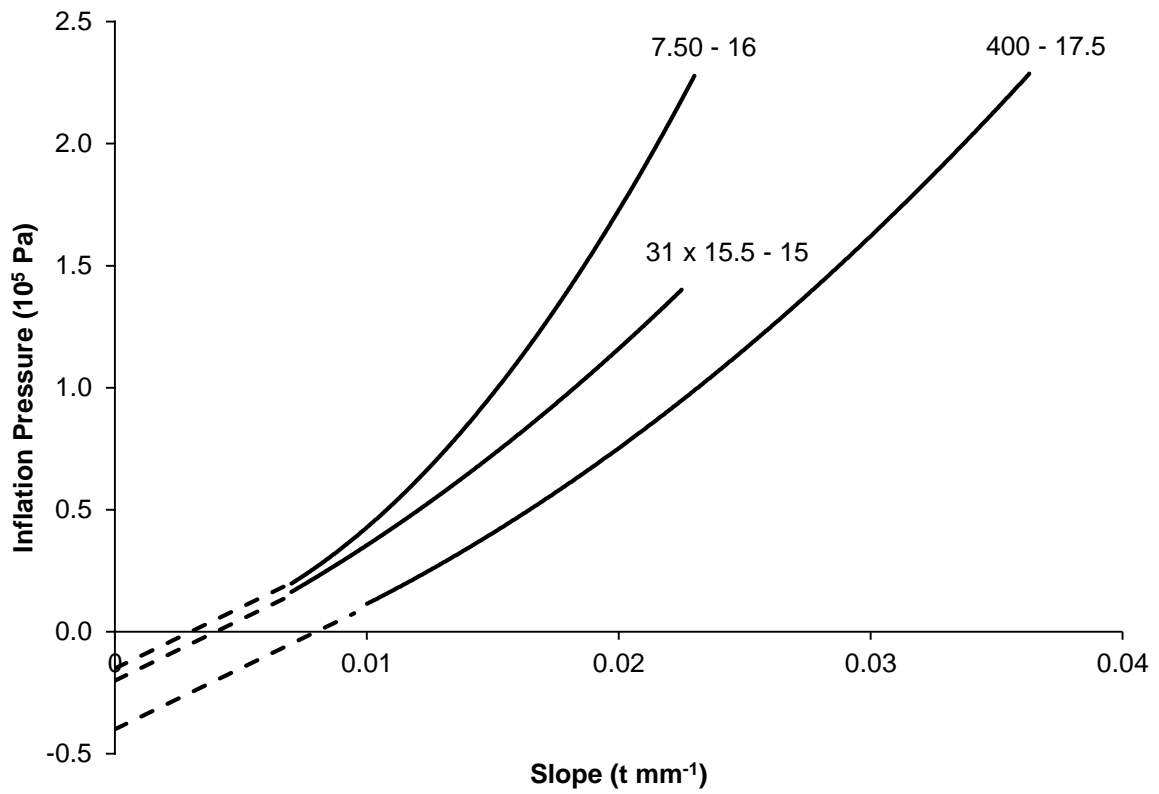
460 Table 1. Comparison of mean carcass stiffness values of the smooth and treaded
461 Trelleborg T421 Twin Implement 600/55-26.5 tyres



462

463 Fig. 1. Load vs. deflection curves for a tyre at a range of inflation pressures (redrawn

464 from Plackett, 1983)



466

467 Fig. 2. Carcass stiffness estimation from the inflation pressure vs. slope of load –

468 deflection curves for three tyres (redrawn from Plackett, 1983)



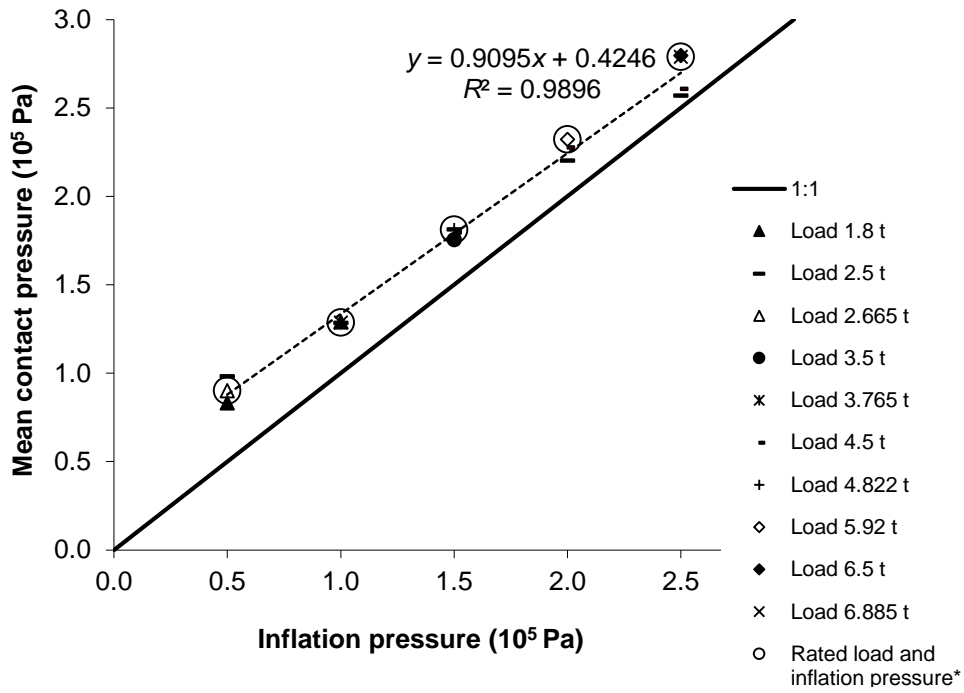
483

484 Fig. 3. Soil bin laboratory (a: soil surface preparation, b: pressure mapping system
485 placed on the steel plates)

486
487
488
489
490
491
492
493
494
495
496
497
498
499
500
501
502
503
504
505
506
507
508
509
510

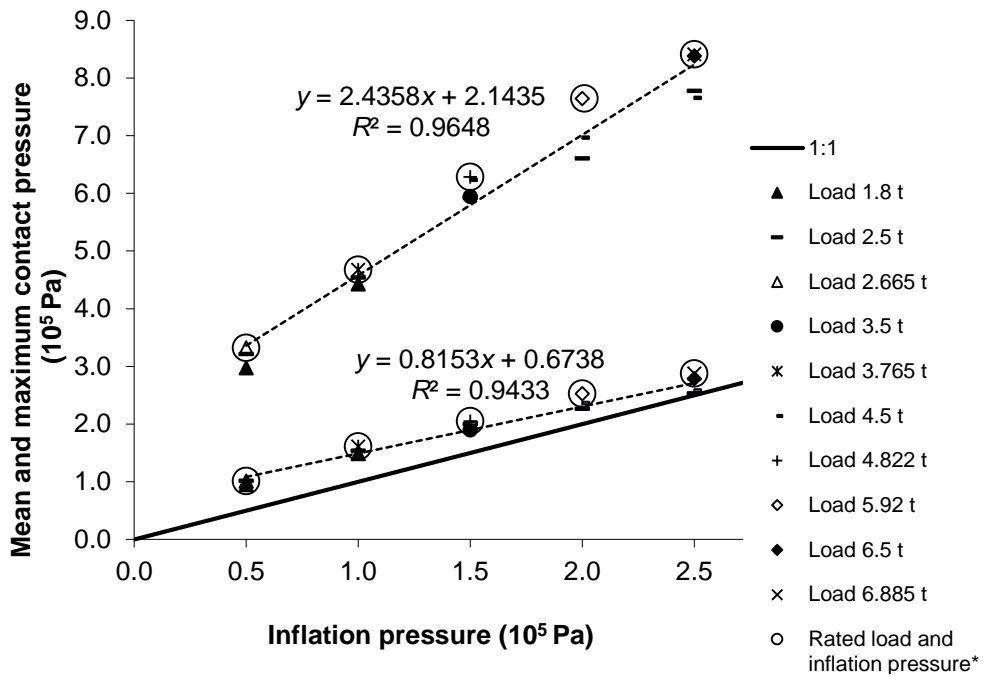


Fig. 4. Smooth (a) and treaded (b) Trelleborg T421 Twin Implement 600/55-26.5
tyres



511

512 Fig. 5. Mean contact pressure vs. inflation pressure for the smooth 600/55-26.5
 513 implement tyre from the footprint area method (*the single marker centred within
 514 each circle indicates a data point for a rated combination of load and inflation
 515 pressure)



516

517 Fig. 6. Mean and maximum contact pressure vs. inflation pressure for the 600/55-
 518 26.5 treaded implement tyre from the footprint area method (*the single marker
 519 centred within each circle indicates a data point for a rated combination of load and
 520 inflation pressure)

521

522

523

524

525

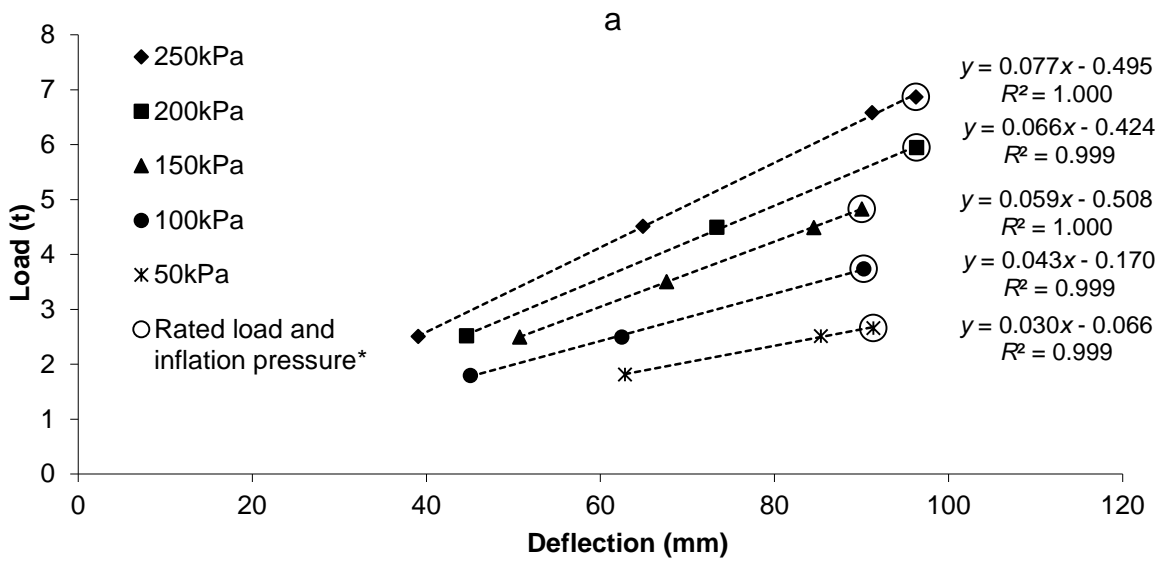
526

527

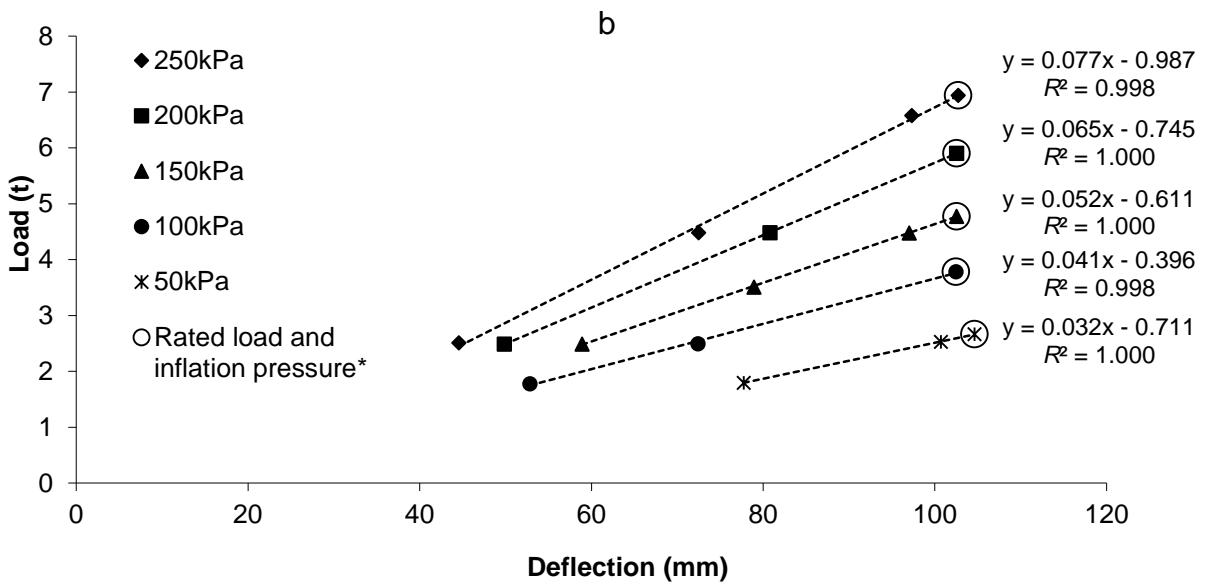
528

529

530



531

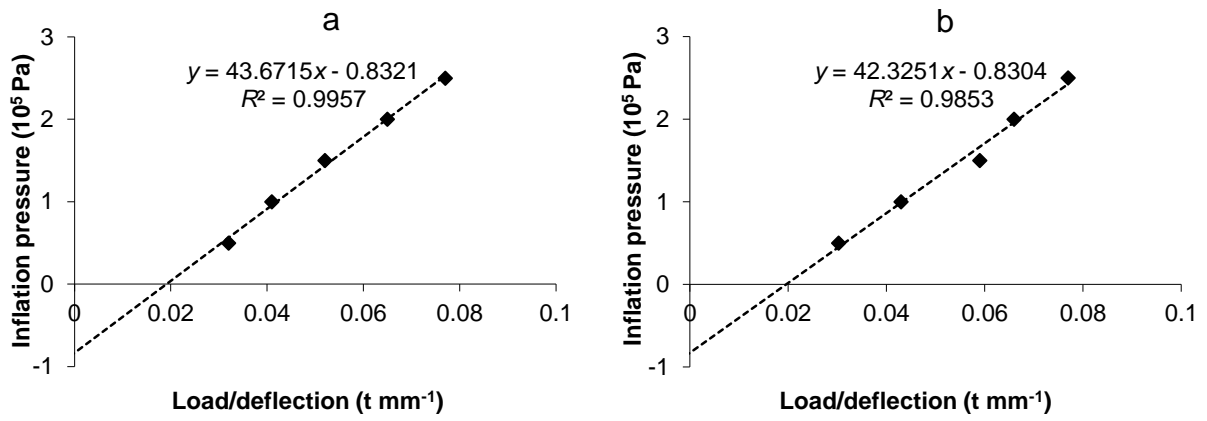


532

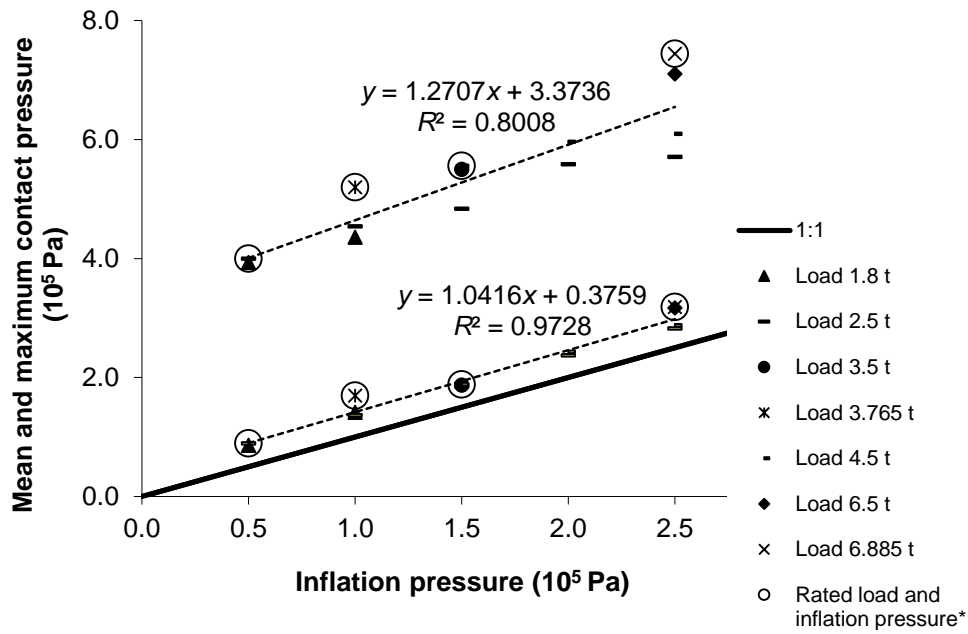
533 Fig. 7. Load vs. deflection curves – smooth (a) and treaded (b) 600/55-26.5

534 implement tyre (*the single marker centred within each circle indicates a data point

535 for a rated combination of load and inflation pressure)



537 Fig. 8. Inflation pressure vs. slope of load – deflection curve – smooth (a) and
 538 treaded (b) 600/55-26.5 implement tyre



539

540 Fig. 9. Mean and maximum contact pressures vs. tyre inflation pressure for the
 541 smooth 600/55-26.5 implement tyre for a range of safe working loads based on the
 542 pressure mapping system (*the single marker centred within each circle indicates a
 543 data point for a rated combination of load and inflation pressure)

544

545

546

547

548

549

550

551

552

553

554

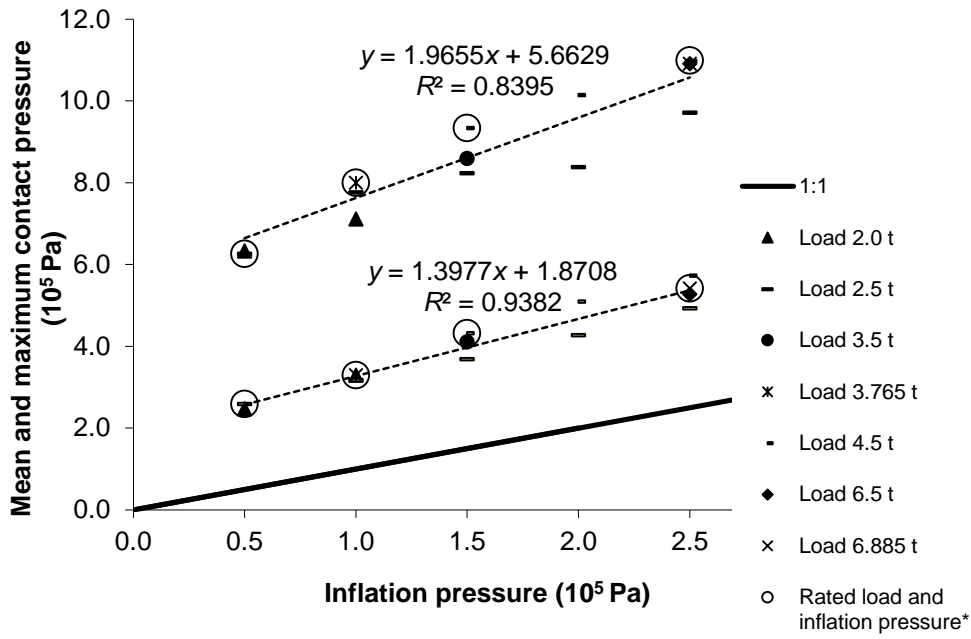
555

556

557

558

559



560

561

562

563

564

565

566

567

568

569

570

571

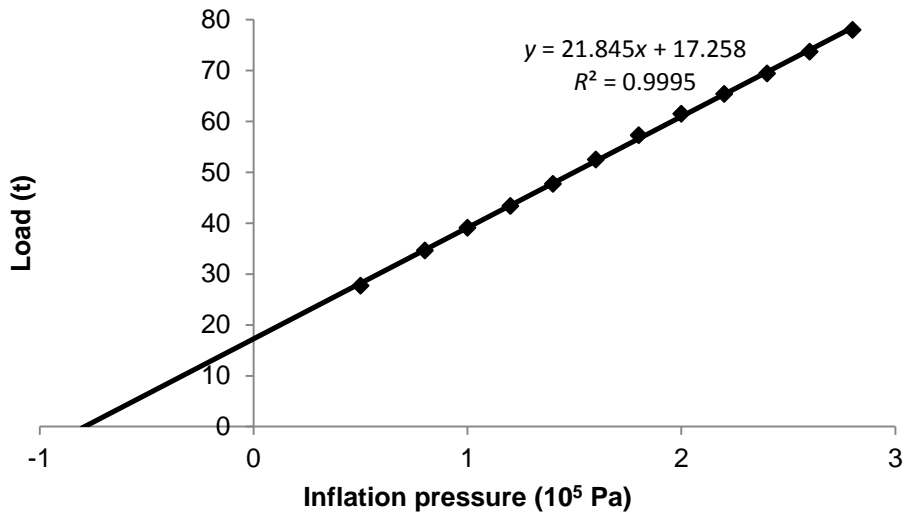
572

573

574

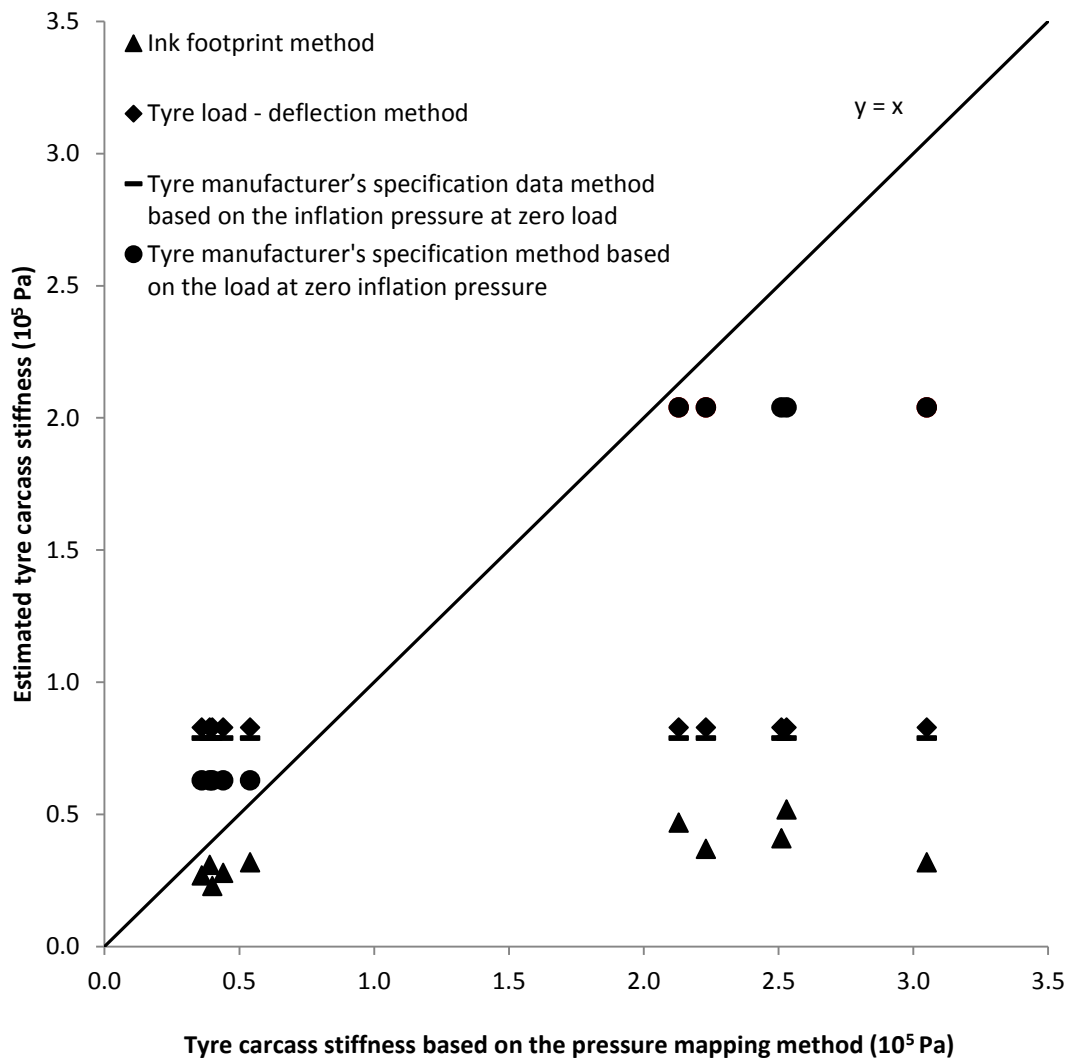
575

Fig. 10. Mean and maximum contact pressures vs. tyre inflation pressure for the treaded 600/55-26.5 implement tyre for a range of safe working loads based on the pressure mapping system (*the single marker centred within each circle indicates a data point for a rated combination of load and inflation pressure)



576

577 Fig. 11. Tyre manufacturer's specification data showing the inflation pressure vs.
 578 load with a linear regression function for the 600/55-26.5 implement tyre (free rolling
 579 at 10 km h⁻¹ speed)



581

582

583

Fig. 12. Comparison of the mean estimated tyre carcass stiffness values with absolute measured values for the Trelleborg T421 Twin Implement 600/55-26.5 tyres

584 Table 1. Comparison of mean carcass stiffness values of the smooth and treaded Trelleborg T421 Twin Implement 600/55-26.5
 585 tyres

Tyre	Pressure mapping method		Footprint area method		Load – deflection method P_{CS} (10^5 Pa)	Tyre manufacturer's specification method at 10km h ⁻¹	
	Overall mean P_{CS} (10^5 Pa)	P_{CS} at rated load and pressure (10^5 Pa)	Overall mean P_{CS} (10^5 Pa)	P_{CS} at rated load and pressure (10^5 Pa)		P_{CS} An inflation pressure at zero load (10^5 Pa)	P_{CS} A load at zero inflation pressure (10^5 Pa)
600/55-26.5 smooth implement tyre	0.44	0.54	0.28	0.32	0.83	0.79	0.65
600/55-26.5 treaded implement tyre	2.51	2.53	0.41	0.52	0.83	0.79	2.12

586
 587
 588